*energies*

*Article*

# Fuel Cell Trucks: Thermal Challenges in Heat Exchanger Layout

**Christian Doppler * and Benedikt Lindner-Rabl**

Energy Efficiency & Human Centered Systems Department, Virtual Vehicle Research GmbH, 8010 Graz, Austria
* Correspondence: christian.doppler@v2c2.at

**Abstract:** Fuel cell powertrains have higher efficiencies compared to internal combustion engine powertrains, but—despite lower thermal losses—thermal requirements are noticeably higher. The commonly used Polymer Electrolyte Membrane Fuel Cell is highly sensitive to temperature deviations; hence specifications of coolant temperatures must be strictly observed. Furthermore, their working-temperature level is closer to ambient air, requiring a more efficient cooling system. This work focuses on medium-duty and heavy-duty truck segments. The aim is to provide a possible optimization guideline for cooling system developers to select an adequate heat exchanger for available air mass flows. This energetical and thermal layout process is based on fuel cell module information provided by Plastic Omnium New Energies Wels GmbH, firstly by simple steady-state calculations and secondly by transient vehicle system simulations. To define the system to the full extent, the analyses cover full-load operation, VECTO cycles, real-driving cycles, and the highest ambient temperatures. Finally, an optimized system is presented, matching the best trade-off between heat exchanger size and mass flows. Results show a linear and then exponential increase in heat exchanger size with soaring thermal requirements. Thus, with a well-defined thermal layout validated on the full vehicle level, the lowest possible component sizes are identified at which still harshest mission profiles can be completed.

**Keywords:** fuel cell electric truck; front-end HX; thermal management; heat exchanger sizing; high voltage fan



**Citation:** Doppler, C.; Lindner-Rabl, B. Fuel Cell Trucks: Thermal Challenges in Heat Exchanger Layout. *Energies* **2023**, *16*, 4024. https://doi.org/10.3390/en16104024

Academic Editor: Remzi Can Samsun

Received: 30 March 2023
Revised: 28 April 2023
Accepted: 4 May 2023
Published: 11 May 2023



## 1. Introduction

### 1.1. FC Energy Balance

Current FC truck applications (realized or in development), that are above 30 t gross vehicle weight (GVW) are usually powered by 2 FC stacks, that have very roughly a system power of 200–300 kW. FC trucks below 30 t gross weight can be equipped with a single FC stack, which means approximately 100–150 kW system power (For details see Pardhi S. et al. in [1] with a list of current and upcoming FC electric long-haul HD truck initiatives). In this Section 1, based on FC system studies or FC system demonstrators, numbers on stack efficiencies, system efficiencies, and thermal losses are summarized and reported for a coarse evaluation of power shares in FC HD truck application (see summarized in Figure 1). The FC stack efficiency curve is highest at part load operation (very low electrical currents) and decreases linearly at high loads (increased current in cells) due to raised activation losses, ohmic losses and concentration losses. In contrast, the FC system efficiency curve is lowest at the beginning of FC load range due to predominant auxiliaries' consumption. It reaches a maximum in the center load area before slightly falling again due to a possible exponential increase in the auxiliary's consumption (mainly air compressor) [2]. A PEMFC has approximately 50% efficiency on average [3], hence 50% of the energy from the hydrogen is losses and needs to be dissipated by the FC system. According to the work from Schnorpfeil S. et al. in [3], this can be split up into 5–10% exhaust enthalpy, 40–45% coolant, 5% charge air cooling, and 3.5% convection and radiation heat to ambient air. In a conference paper from 2021 in [4], Symbio as an FC system manufacturer presents a study on FC driveline for HD trucks with 350 kW wheel power, 567 kW losses, 507 kW stack heat to coolant (89% of losses), 29 kW charge air heat power (5% of losses), and 31 kW exhaust heat (6% of losses). Further, the main HX requirements are compared to a similar ICE driveline [4]: ICE driveline with 240 kW coolant losses @ 105 °C vs. FC driveline with 508 kW coolant losses @ 85 °C, showing up the specific challenge to design an appropriate HX. Aschauer T. and Schutting E. from TU Graz presented in 2022 in [5] a share of exhaust enthalpy of about 5–10% and a 91% share of excess heat removed by coolant. It is remarked a slightly higher efficiency of FCs at the nominal load point of around 10–20% compared to ICE but due to reduced exhaust enthalpy, the heat dissipation via the coolant system ends up being 40–50% higher. The lower heat losses in the exhaust are mainly because of the very low exhaust temperatures of around 60 °C [6]. In [7], Linderl J. from AVL presents their FC system for HD trucks with an FC system rated power of 308 kW Begin of Life (BOL) and 272 kW End of Life (EOL) at an FC system efficiency of 44.8% at rated power (BOL) driving an e-axle with 360 kW max. cont. power and 540 kW max. peak power. This would approximately lead to 380 kW thermal losses (BOL), which additionally increase with an aged FC system. Ref. [8] reports about this additional challenge in heat rejection with FC at EOL. Here, an example is given with a 20% efficiency decrease (worst-case) which requires shifting the load point towards a higher voltage to provide the same electrical energy. The additional heat that must be rejected increases in that case by +60%.

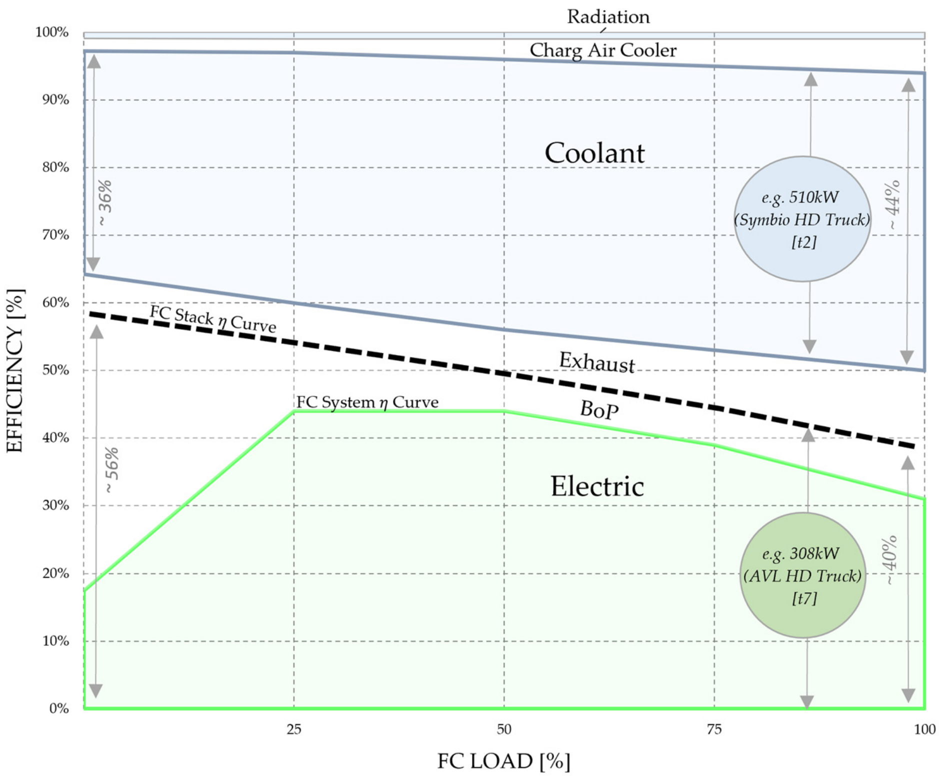


**Figure 1.** Efficiency vs. FC Load with Energetical Shares.

In [9], a Sankey diagram shows simplified the share of FC energy flow which is 6% exhaust, 42% coolant, and 52% electric.

Figure 1 summarizes the power flow shares in a conventional FC system (based on efficiency and FC load) upon the described literature. Electrical energy share is represented below the dashed line with the system net output in green and the BoP (Balance of Plant) share. The thermal energy share is above the dashed line with shares of exhaust enthalpy, charge air cooling, radiation, and coolant, distinctly showing the huge share of energy going into the coolant.

*1.2. FC Thermal Management*

The thermal management for a PEMFC requires a liquid cooling loop, see Figure 2. An HV pump provides coolant mass flow across the bypass or the HX, which is controlled via the 3-way valve. The cooling air flow can be increased with the HV fan. In FCEVs, the process air is directed separately across a, which allows the FC to provide the required amount of air, hence oxygen starvation is no critical issue in these applications.

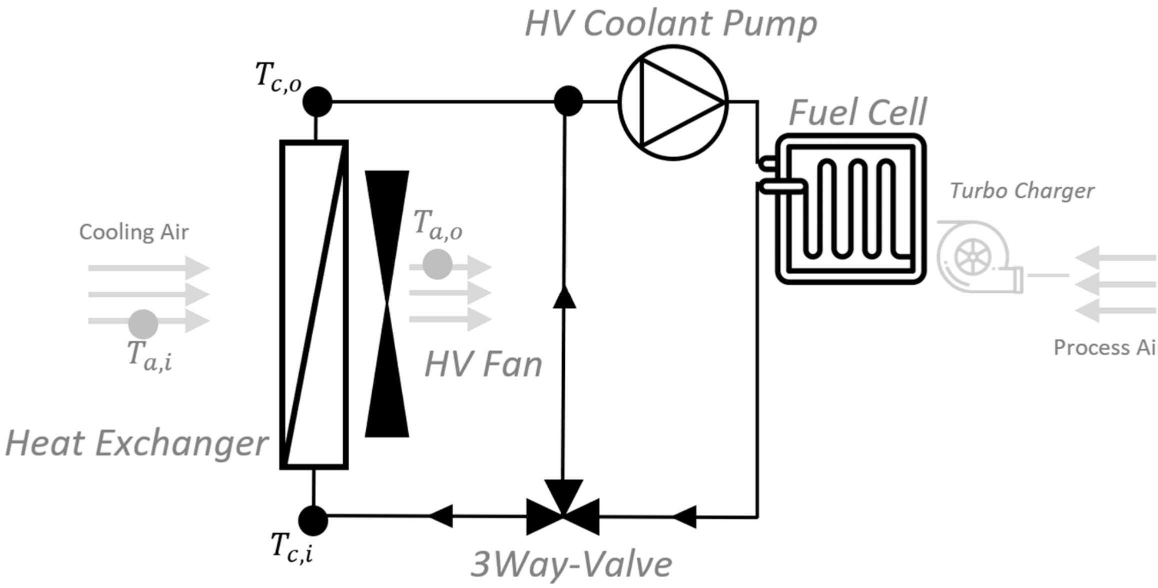


**Figure 2.** FC Thermal Management System.

1.2.1. Temperatures for Cooling the FC

FCs for HD trucks are specified for ~25,000–30,000 h of operation [2]. For the protection of the cells, several measures such as limited transient operation and precise compliance with target temperatures are indispensable. In terms of thermal management, basically, a similar cooling system such as an ICE-operated truck is used. Via a cooling loop, heat is transported to a cross-flow main HX and dissipated to the ambient air. Air flow enters air inlets and passes the HX before crossing the under-bonnet area. For support, a fan is activated to increase the air flow. The pressure losses across the HX and the under-bonnet area strongly influence the air flow. Possible measures to improve the air heat transfer are using a bigger cross-sectional area or an increased depth (the latter only to a certain extent as described later).

The main driving force for a high heat flow is the temperature difference of coolant to air. When looking at an ICE driveline, coolant temperatures can be in the region of 90–120 °C [3]. For an FC driveline, the temperature region is very little and much lower with a small window at around 80 °C average temperature [3]. Especially at higher ambient temperatures, the reduced delta between coolant and ambient air is crucial and needs extra attention. In the doctor's thesis from Berger O. in [3], coolant inlet- and outlet-temperatures are reported in the region of 64–77 °C, with ~55 L/min coolant flow for an FC passenger car which is driving on the Großglockner Pass Road. When the inlet temperature reaches 72 °C, the fan is activated, at 78 °C, FC stack power is reduced, at 80 °C, the FC is shut off to prevent damage. The stack coolant temperature difference is defined and constantly controlled to a value of 5.5 K. These concrete numbers descriptively show the maximum thermal working area of an FC. In [10], Pietruck M. from RWTH Aachen presents a thermal FC system design with an inlet coolant temperature of 70 °C which is controlled via a bypass valve. It reported an FC shut-off event at 90 °C coolant temperature to prevent component damage. Roiser S. from TU Graz reports in [11] an FC system with inlet-and outlet temperatures of 70 °C and 75 °C, respectively. In the region of 75–77 °C, an overheating mode reduces FC power output, above 77 °C, the operation is forbidden.

#### 1.2.2. HX Size for Cooling the FC

Compared to an ICE system, the increased thermal loads in the coolant combined with the lower temperature difference of coolant to ambient air require an increase of HX size and air mass flow. A standard ICE HX for an HD truck has a cross-sectional area of ~0.7–1 $m^2$ [12,13]. In the 2021 work from Roiser S. in [11], a study on an HX size variation for an FC MD truck is presented. For a heat quantity of 126 kW, a 1.3 $m^2$ big HX cross-sectional area is chosen at an ambient temperature of 40 °C and a temperature difference of 35 °C. A strong nonlinear increase of HX cross-sectional area is reported when the temperature difference is reduced even more, e.g., to a difference of 30 °C, ending up in an HX cross-sectional area size of above 3 $m^2$. In [12], by Linderl J., an AVL List FC HD truck development is presented in 2021. Moreover, a standard HX from an ICE truck, and an additional (~half in size) HX were mounted. The overall HX cross-sectional area ended up being 1.2 $m^2$. In the work from Aschauer T. in [5], HX frontal area variation is made for an FC-operated telehandler. As a result, compared to the conventional HX for the ICE driveline, it is reported that the FC HX needs to be increased at least by a factor of 1.8. Ref. [11] reports that most of the waste heat goes to coolant and that radiator-specific heat rejection and, therefore, required cooling performance is 1.5–2 times higher compared to the ICE engine. Mayr K. presents in [6] a technical analysis for the future-proof operation of FCs in HD trucks that brings up even a minimum increase of 2.5 times the HX cross-sectional area to cope with high thermal loads in the coolant. In [13], a louver fin heat exchanger for FCEVs is optimized by a genetic algorithm. The dynamic characteristic of improved designs was then evaluated in cycle simulations reporting improved heat transfer rates in the range of 1.6–5%.

#### 1.2.3. Mass Flows for Cooling the FC

In order to fulfill required heat rejection rates and temperature levels, raised coolant and air mass flows are required with low HXs pressure drops. Very good examples of typical FC mass flow areas at relevant operation temperatures (important for heat flow calculation) can be found in the thermal management software KULI from Magna [14].

In KULI software, modelled HXs are usually map-based, created from measurements. Three relevant HXs are presented in Figure 3 all measured with a coolant inlet temperature of 80 °C at an air inlet temperature of 25 °C. For each HX, two different coolant mass flows are shown, restricting with lower dashed curve and upper solid curve the colored working area in the diagram. The blue and the green area represent MD HXs with air mass flows up to 9 kg/s, allowing them to dissipate up to 250 kW of heat for typical operating conditions. The grey area represents a passenger car HX, with air mass flows up to 3 kg/s, and heat quantities up to 100 kW that can be dissipated.

#### 1.2.4. Auxiliaries Loads for Cooling the FC

The required air mass flows can be guaranteed using a high voltage (HV) fan. Due to the required very high mass flows and required high depth of the HX, high electrical loads result. In the presentation in [4], during the design phase of an FC HD truck, the assumption of a maximum fan power of 30 kW was made. In the HyTruck project led by AVL, maximum fan powers up to 40 kW are reported [7]. Parameter studies for 11–42 kW electrical fan power are presented in [12]. In [15], FC systems for heavy-duty vehicles are studied and high thermal loads from FC are proposed to be solved either with increased battery energy supply or with improved radiator design. In these analyses, the fan power is calculated by the Multiwing Optimizer accounting for a 30 kW electrical load. In a report from AVL List & ZSW in [6], as a drawback of an FC system, a potential fan power of up to 60 kW is mentioned, meaning this could be seriously scorching FCs in automotive applications. The industry is currently bringing HV components to the market, such as:

- EMP HV front-end fan, max. 25 kW electric energy consumption [16]
- EMP HV coolant pump, max. 3 kW electric energy consumption [17]
- Borg Warner HV front-end fan, max. 40 kW electric energy consumption [18]
- Rheinmetall HV coolant pump, max. 2.2 kW electric energy consumption [19]

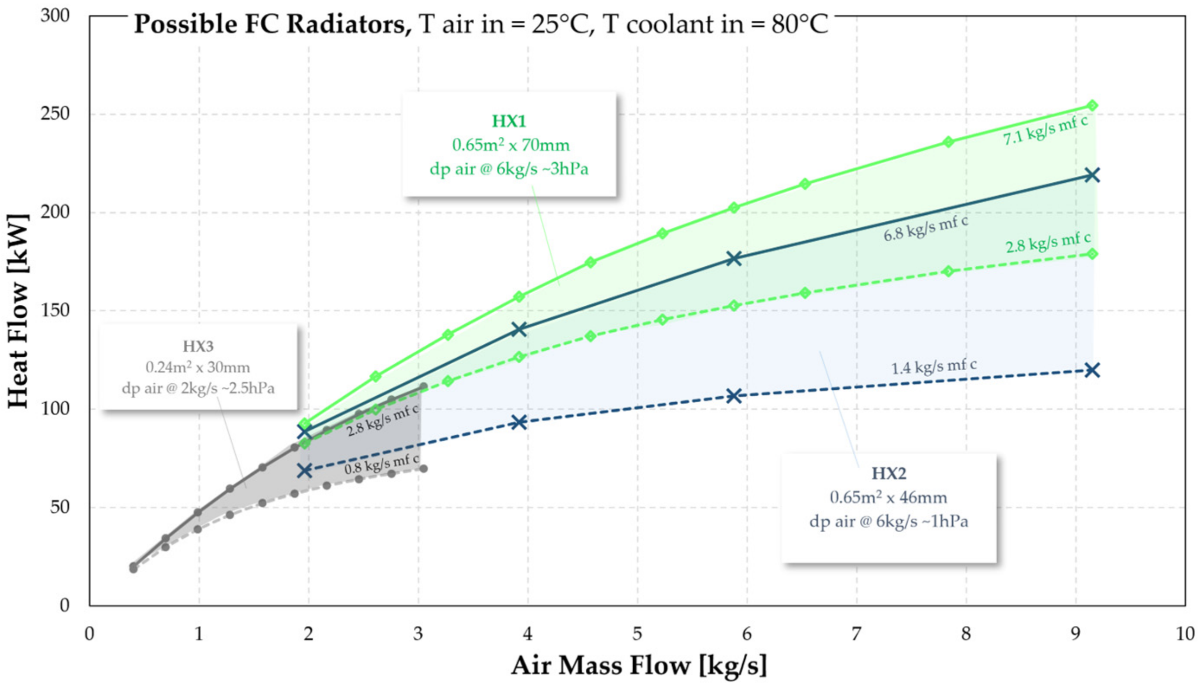


**Figure 3.** Heat flow versus Mass Flow for Possible FC HXs, Data from KULI Software [14].

Ref. [20] reports the thermal management layout for an FC system in the towing test on Davis Dam at 40 °C ambient temperature concluding that a careful design trade-off for an air of radiator must be made on: (i) fin density, fan selection, and cooling air flow, (ii) heat balance amongst radiator, and (iii) design feasibility for production parts. A high-power fan is especially required for low vehicle speeds.

As described in the sections above, scattered information on FC thermal management is available with unique examples. In general, no common scheme for the layout process nor a general guideline is available, hence, this publication tries to fill up this gap.

## 2. Methodology

The methodology is described in an overview in Figure 4. In the first phase, inputs are collected. As the first input, the vehicle type is defined to identify the operational area (temperatures) and required FC power. Relevant FC parameters such as maximum power output and thermal output are collected. As the next input, parameters on the thermal system are collected or defined such as possible sizes for HX integration or the electric load range for the fan. The thermal equations are constituted as the last input for the upcoming calculations.

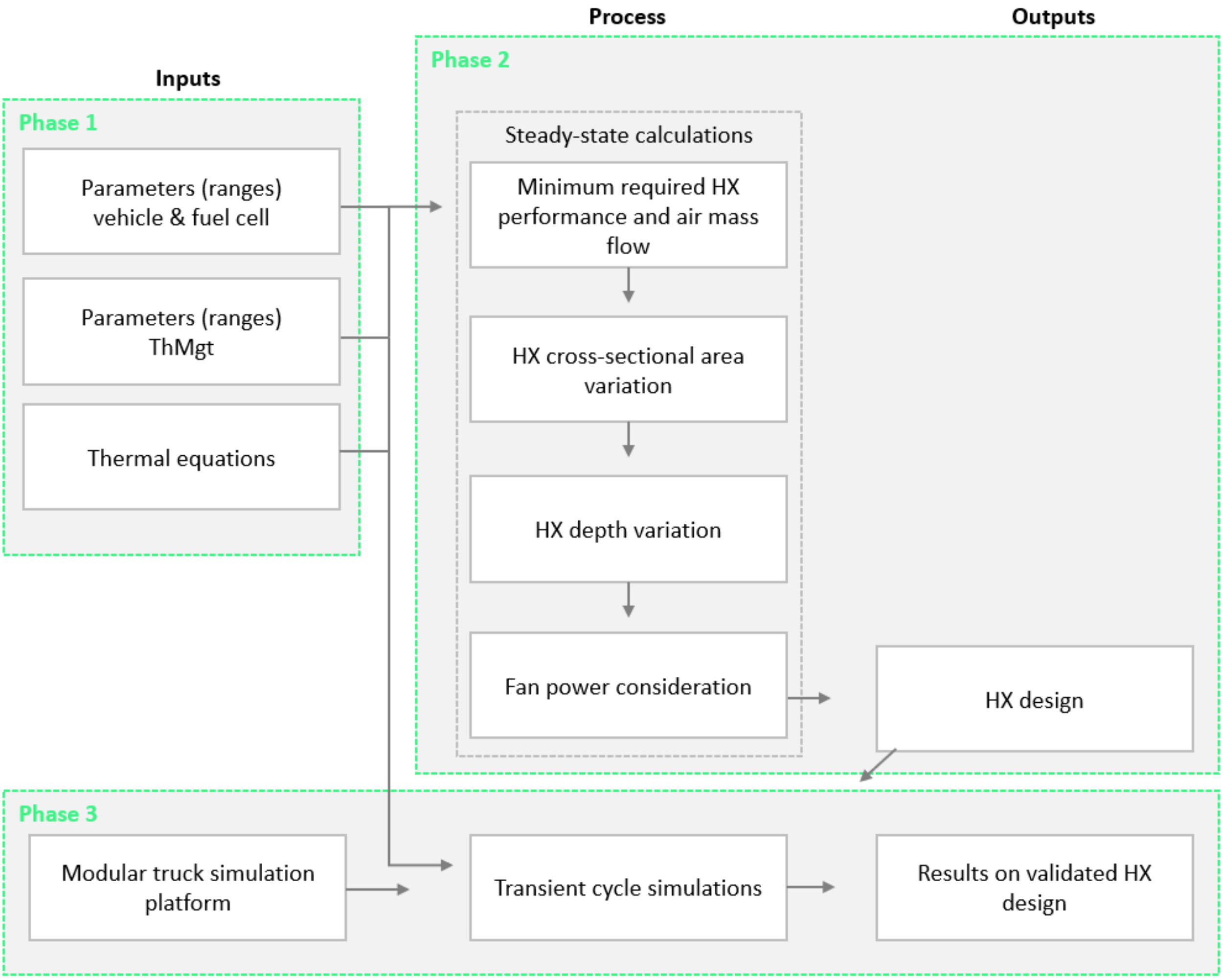


**Figure 4.** Methodology and Process Description of this Work.

In the second phase, design steps based on steady-state calculation are examined. For the maximum heat flows at defined ambient temperatures, the minimum requirements are evaluated. Next, variations on the HX design are assessed to identify the best trade-off between all the relevant parameters. Last, considerations on the fan power consumption are presented for an altogether examination. The HX design is an output of phase 2.

In the third phase, a modular truck simulator platform is used and the designed HX and fan are integrated. By conducting transient cycle simulations, results on validated HX design are presented.

### 2.1. Parameters for FC and Vehicle

As a starting point for the layout process of FC thermal management, the reference vehicle classes are defined. In detail, MD and HD truck classes are investigated for the definition of suitable HX sizes and air mass flows. For these classes, different FC system sizes are considered, with the properties summarized in Table 1. This data is based on fuel cell information from Plastic Omnium New Energies Wels GmbH in the research project NextGenFCM, from which this publication originates.

**Table 1.** Main Vehicle and FC Parameters.

| Parameter | Medium Duty | Heavy Duty | Unit |
|---|---|---|---|
| Gross Vehicle Weight (GVW) | 26 | 40 | t |
| # FCs | 1 | 2 | - |
| $\dot{Q}_{FC}$ @ full load | 200 | 400 | kW |
| Temperature spread of coolant | 0.05 | | $K/kW_{th}$ |
| Target temperature coolant, FC, in | 62–70 | | °C |
| Target temperature coolant, FC, out | 63–80 | | °C |
| Efficiency @ part load | | >60 | % |
| Efficiency @ full load | | <50 | % |
| Mass flow coolant | 1–6 | 2–12 | Kg/s |
| Temperature ambient max. | 45 | | °C |

## 2.2. Parameters for Thermal Management

Table 2 below lists the main thermal parameters with relevant value ranges for designing, evaluating, and optimizing the FC cooling circuit. The most important component is the front-end HX, whose size, and thus performance, depends on the available packaging of the vehicle. As a starting point, its dimensions are taken directly from components of a comparable ICE-operated HD truck. A typical European HD truck is considered, such as a Volvo FH class or Scania S class. In conjunction with the HX, a fan must be also defined that can supply the appropriate air mass flow at a given air resistance to ensure a high heat dissipation. According to the thermal requirements of the FC, a coolant pump for high-mass flows is required. Finally, see all the defined specifications in an overview in Table 2 below.

**Table 2.** Main Thermal Management Parameters.

| Parameter Group | Parameter | Range | Unit |
|---|---|---|---|
| HX [21–23] | Width | 800–1000 | mm |
| | Height | 600–1000 | mm |
| | Depth | 40–143 | mm |
| Fan [16] | Electrical power | ≤25 | kW |
| | Blade diameter | 780 | mm |
| | Air volume flow | 9 | $m^3/s$ |
| | Pressure increase | 1000 | Pa |
| Coolant Pump [17] | Electrical power | ≤2.3 | kW |
| | Internal propeller diameter | 100 | mm |
| | Coolant volume flow | 4.7 | l/s |
| | Pressure increase | 1.5 | bar |

With the identified parameters, sufficient information is available to fully parameterize the thermal management of the FC system. The HX energy balance can be established with the knowledge of all boundary conditions on the coolant side and the air side. The next step is to define the test scenarios under which the thermal system will be designed and the methodology by which the system will be evaluated.

## 2.3. Thermal Equations

The waste heat flow $\dot{Q}$ of the FC stack coolant circuit is dissipated to the ambient air via the HX. This coupling of coolant and air is described by Equation (1),

$$\dot{Q} = k * A_{HX} * \left(\overline{T}_{coolant} - \overline{T}_{air}\right) \tag{1}$$

where $k$ = overall heat transfer coefficient in $W/m^2K$, $A_{HX}$ = overall heat transfer area in $m^2$, $\overline{T}_{coolant}$ = mean coolant temperature HX in °C and $\overline{T}_{air}$ = mean air temperature *HX* in °C. It discloses the coolant and air temperature difference as the driving force of heat transfer. Equation (2) shows the calculation of a linearly assumed mean temperature $\overline{T}$ in °C,

$$\overline{T} = \frac{T_{out} + T_{in}}{2} \tag{2}$$

where $T_{out}$ = outlet temperature in °C and $T_{in}$ = inlet temperature in °C. Equation (1) can be rewritten to Equation (3), to better describe the thermal conductance of the $HX$. As described, $k$ is the heat transfer coefficient, which is composed of the convective heat transfer on the coolant side, the heat conduction in the material from the coolant side to the air side, and finally, the convective heat transfer on the air side, and $A_{HX}$ is the available heat transfer surface.

$$k * A_{HX} = \dot{Q}/(\overline{T}_{coolant} - \overline{T}_{air}) \tag{3}$$

The left side of Equation (3), namely the HX conductance $k * A_{HX}\left[\frac{W}{K}\right]$, is representing a kind of fictitious "HX-performance value", which can be used to compare different HXs. Next, Equation (4) describes in detail the air side convective heat transfer which contributes to $k$. The direct influence and the relevance of the air mass flow on the heat transfer can be seen in Equation (4). By combining with Equation (3), Equation (5) can be established, in which all the relevant influencing parameters for heat transfer are identified.

$$\dot{Q} = \dot{m}_{air} * c_{p,air} * \Delta T_{air} \tag{4}$$

$$k * A_{HX} = 1/\left[\frac{1}{\dot{Q}} * \left(T_{c,i} - T_{a,i} + \frac{\Delta T_c}{2}\right) - \frac{1}{2\dot{m}_{air} c_{p,air}}\right] \tag{5}$$

where $\Delta T_{air}$ = temperature difference of the air in $K$, $c_{p,air}$= specific heat capacity of air in J/kgK, $\dot{m}_{air}$= mass flow of air through $HX$ in kg/s, $T_{c,i}$ = inlet temperature of the coolant in °C, $T_{a,i}$ = inlet temperature of the air at $HX$ in °C and $\Delta T_c$ = coolant temperature difference in K.

### 2.4. Modular Truck Simulation Platform

A modular truck simulator is developed and used to validate thermal management on the full vehicle level. It consists of FC truck-specific submodules (longitudinal dynamics, eAxle, power electronics, FC system, battery storage, cooling circuits, controls, and driver) and it is built in MATLAB/Simulink environment.

The simulator mainly involves the setting of major vehicle parameters such as frontal area size, GVW, drag coefficient, dynamic rolling friction coefficient, battery size, EM size, etc. These parameters are defined and selectable for HD or MD trucks.

On one side, it is important to show accurately the interaction of mechanical, electrical, and thermal systems. On the other side, the final and main modelling target is to evaluate the behavior of the thermal system in the full vehicle context during stationary high-load operation and dynamic driving cycles. An overview of the submodules and their physical domains is given in Figure 5 and in Table 3.

In the submodule cycle, vehicle target speed and road inclination are the base inputs for the used forward approach or so-called dynamic approach to calculate the vehicle dynamics in a further step. In the driver submodule, with PI control, gas pedal, and brake pedal actions are calculated and as a further consequence, a desired torque is provided. These are then passed on to the longitudinal dynamics submodule which interacts with the rest of the subsystems. Powertrain Energy Management (PEM) is basically a function of the ESS state-of-charge (SOC). The lower the SOC, the higher the requested FC power. This allows keeping the SOC usually between 30–60%, hence always having the potential for significant recuperation phases. In general, the focus is put on the rather steady-state operation of FC with fewer start/stop events to prevent the FC from aging. An FC derating mechanism is integrated into the software, but it has been deactivated for the simulations shown below. This allows fundamental analysis in the way of a fairer and clearer assessment of components without influences from specific control mechanisms. In the FC submodule, two modules can be chosen. The first is a map-based FC model (steady-state), the second is a transient FC model for more accurate dynamic system behavior which is modeled and provided by HyCentA Research GmbH in the framework of the NextGenFCM project. In addition to the simulation, a comprehensive post-processing is performed in MATLAB/Simulink for storing and analyzing time-resolved results as well as sum results, see a selection in the next section.

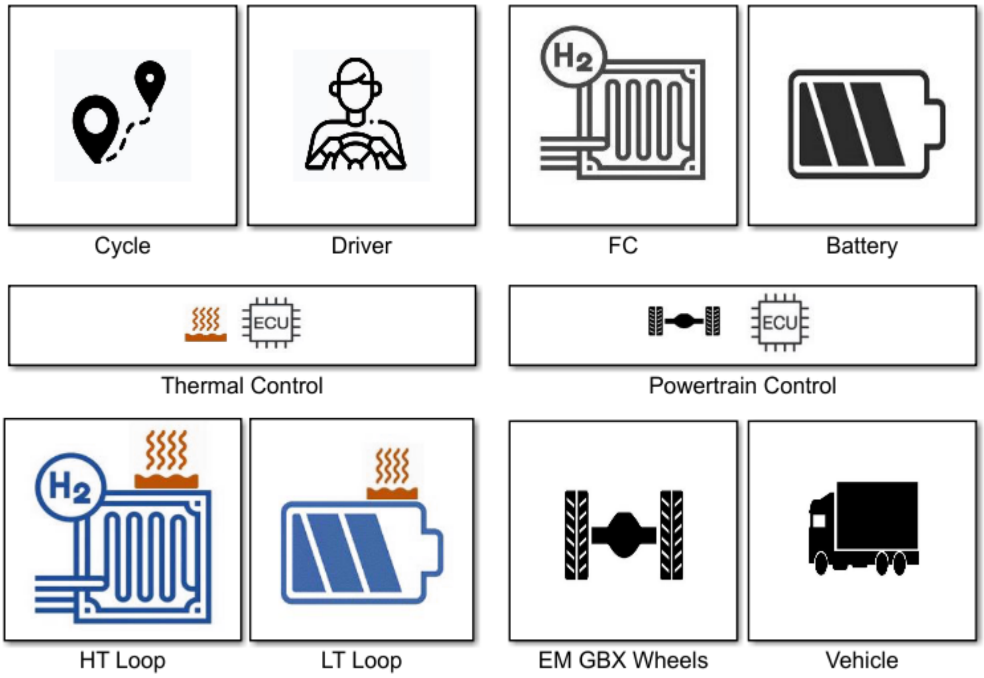


**Figure 5.** Modular Truck Simulator.

**Table 3.** Submodules with Properties.

| Submodule | Mechanical | Electrical | Thermal |
|---|---|---|---|
| e-Axle | yes | yes | yes |
| Gearbox | yes | no | no |
| Longitudinal Dynamics | yes | no | no |
| FC System | no | yes | yes |
| Battery | no | yes | yes |
| Power Electronics | no | yes | yes |
| Cooling System | no | yes | yes |

## 3. Results

### *3.1. Steady-State Calculations*

The thermal management system needs to ensure thermal protection of the FC system under all envisaged operating conditions. This includes also worst-case scenarios such as steady-state FC operation at full load during vehicle standstill at highest ambient temperatures up to 45 °C. Steady-state calculations are conducted at different ambient temperatures in running the FC system at constant loads to evaluate minimum required air mass flows at different HX sizes. In the next step, a variation of boundary conditions is performed to assess the effect on HX surface growth. Basically, no complex simulation is required to answer this question, but it can be already carried out in the design phase of the thermal system with the formulas before.

#### 3.1.1. Minimum Requirements for the HX

In the first step of the HX layout process, the "HX requirements" must be defined. To operate 1 FC at full load in a steady state ($\dot{Q}$ = 200 kW), the minimum required air mass flow can be calculated with the formulas above. The temperatures of the coolant inlet and outlet (fixed due to FC requirements) and air inlet (fixed due to given ambient temperature) are given, only the air outlet can be changed or influenced by the HX. For this calculation, an ideal HX behavior is assumed with an air outlet temperature correlating to the coolant inlet temperature. With this assumption of an ideal behavior, transient effects as well as losses such as radiation are neglected and Equation (5) can be applied without further corrections. The HX conductance $k * A_{HX}\left[\frac{W}{K}\right]$—a key figure for the overall thermal HX performance—can be calculated with Equation (5) for different air mass flows. Finally, Figure 6 shows these results for the FC operation at full load at various ambient temperatures. The minimum required air mass flow as well as the required HX conductance are plotted versus ambient temperature. To dissipate the heat losses of 1 FC at full load in steady state operation, the air mass flow must be in the region of 2–5.5 kg/s with HX conductance values of 7500–16,000 W/K, depending on ambient temperatures; values are for 1 FC in an MD truck. For 2 FCs with heat losses of 400 kW, these "HX requirements" must be doubled.

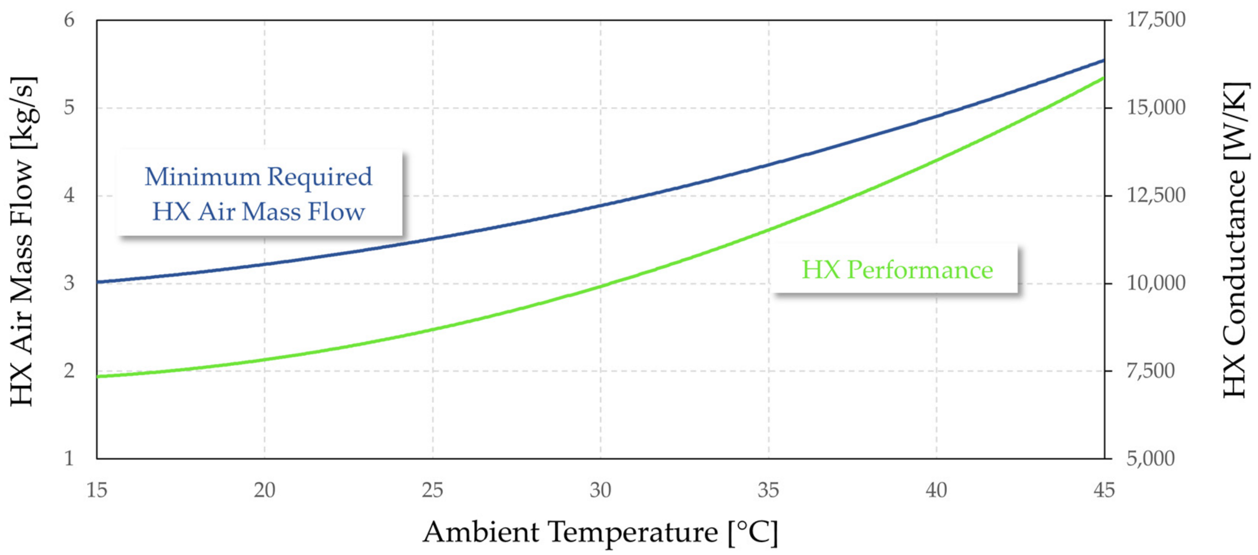


**Figure 6.** Thermohydraulic HX Requirements in an FC MD Truck.

#### 3.1.2. Relation of FC Power, HX Size, and Air Mass Flow

The space for integrating the HX is usually strongly limited, thus the required HX conductance—plotted in Figure 6—may rather deviate from this ideal assumption due to packaging constraints. So, a reduction of the optimum HX size leads to a necessary increase in air mass flow to dissipate the same amount of heat. If the air mass flow can be higher compared to the required minimum air mass flow in Figure 6, several combinations of air mass flow and HX size can be realized to allow FC full load in steady-state operation. This is basically shown in Figure 7 where the blue curve represents the maximum available FC power at steady state for different air mass flows at constant boundary conditions. The yellow curves represent different HX sizes. With very small HX sizes, the FC can't be operated at full load, not even at very high air mass flows; only a very slight increase of possible FC power can be observed. With more HX size and by additionally increasing the air mass flow, the FC can be operated at full load. The statement of the figure with the cross-influences is valid in general for different types of FC and HX setups. The light blue point in the figure indicates the lower limit of air mass flow to constantly operate the FC stack at full load. The higher the ambient temperature, the farther this point moves to the right. It can be shown that not every HX is able to keep the FC thermally stable at full load. The system designer can now prepare such a chart and choose the combination of HX size and air mass flow, that is feasible to integrate into the vehicle in terms of HX and fan dimensions.

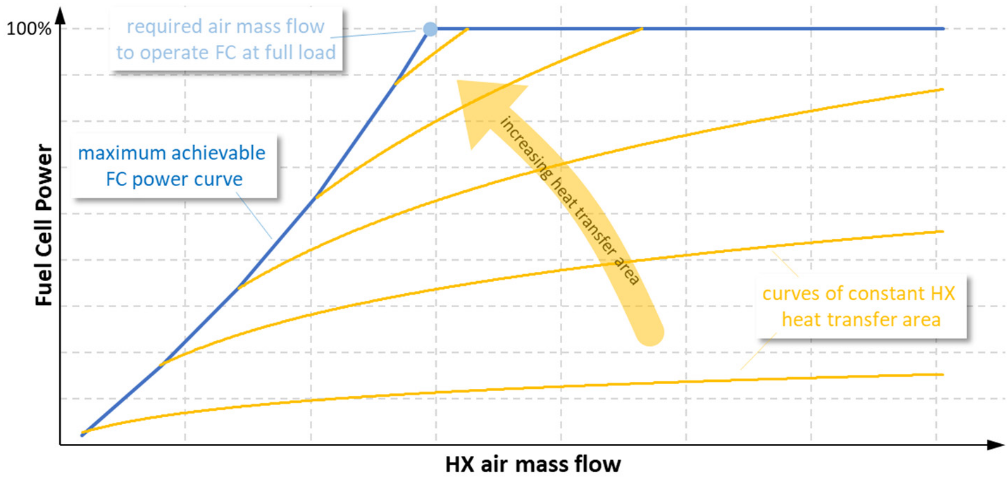


**Figure 7.** Cross Influences of FC Power, HX Size, and Air Mass Flow with FC Power Curve in Blue and HX Size Curves in Orange.

### 3.1.3. HX Size Growth

As a next step, the HX size growth is quantified based on ambient temperature and FC power. By applying Equation (5), a variation of MD truck FC power is made for different ambient temperatures. Equation (5) can be solved for the required HX size, $A_{HX}$ with the resulting curves shown in Figure 8. The curves' non-linearity results from the fact that three of four temperature levels in the system are given fixed ($T_{c,i}$, $T_{c,o}$ & $T_{a,i}$) and, therefore, only $T_{a,o}$ can vary. So, the closer the mean temperatures $\overline{T}_c$ and $\overline{T}_a$ are to each other, the higher is the needed heat transfer area to dissipate heat to the ambient air, which is emphasized by Equation (3). Finally, the non-linearity derives from the reciprocal behavior of the growing temperature difference at the denominator position. As already mentioned, the following limitation is taken into account: $T_{a,o}$ must be lower than $T_{c,i}$.

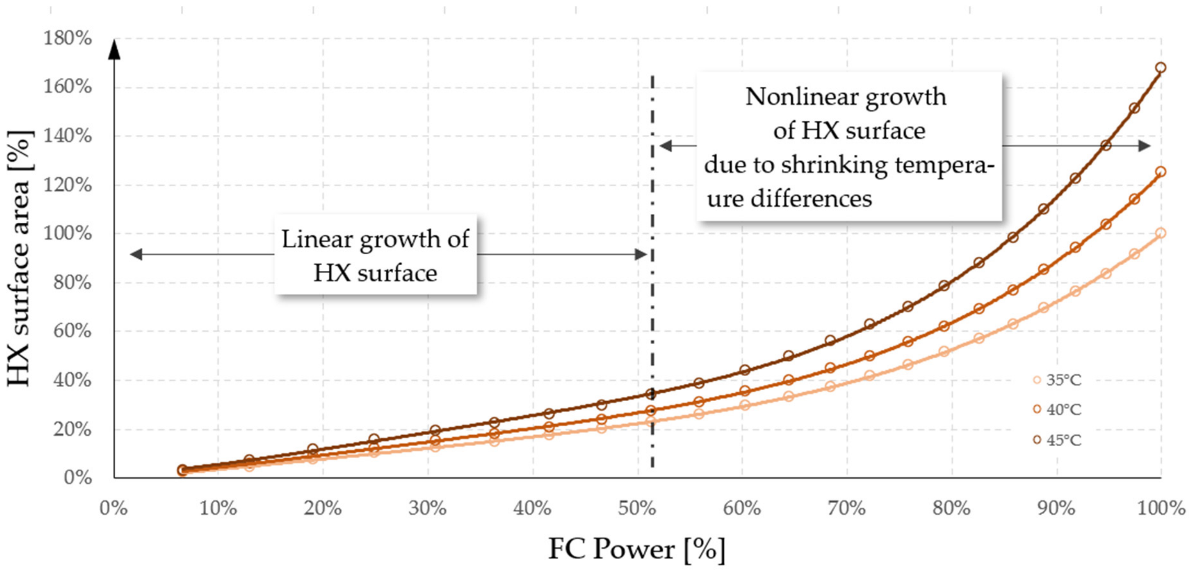


**Figure 8.** HX Size Growth as a Function of FC Power.

Especially for high-temperature conditions, the required HX size is crucial and can become huge in an unpropitious way. Figure 8 illustrates this issue for elevated ambient temperature levels. For ease of illustration, the relative HX cross-sectional area on the ordinate is related to the reference of 35 °C ambient temperature and FC full load. Generating this diagram and calculating absolute values of $A_{HX}$ builds a relevant further step for the system designer to sketch HX growing behavior.

At an ambient temperature change from 35 °C to 40 °C, the HX size must be increased by 25%. If increased up to 45 °C, the necessary HX size grows by about 70% when a constant full load is requested. In general, this behavior is similar also at other temperatures. Up to about 50% FC power, the required heat transfer area grows almost linearly. At higher FC power, due to the increasingly narrow temperature differences, a sharp increase in required HX size can be seen. For example, a change of FC power from 0% to 60% comes along with an HX size change from 0% to 30%. In contrast, the change of FC power from 60% to 100% requires the HX size to increase from 30 to 100%.

### 3.1.4. HX Depth and Fan Considerations

As mentioned, the HX size can't be chosen arbitrarily but must comply with each vehicle's packaging. This is not only relevant for the HX cross-sectional area but also accounts for HX depth. One tempting way to enlarge the overall heat transfer area is to increase HX depth, e.g., by adding a second HX behind the first one in flow direction. Figure 9 gives an example for varying the HXs performance by applying various sets of cross-sectional area and depth. These values are valid for an MD truck operated with 1 FC; each curve represents the limiting FC power for a specific set of HX size and ambient temperature. Again, with an increase in ambient temperature or required FC power, the HX depth increases at a constant cross-sectional area.

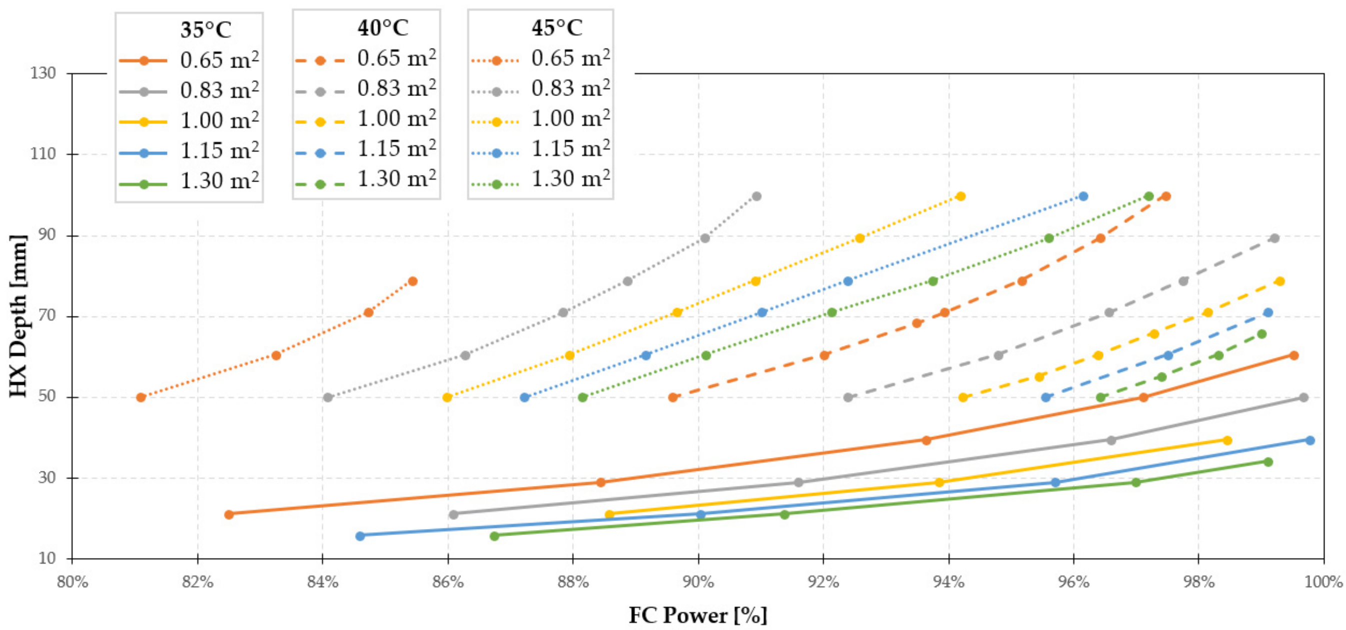


**Figure 9.** HX Size Variations for Various Maximum FC Steady-State Operations.

An increase in HX depth appears to be an appealing solution. Even with enough available space in the vehicle for integrating an HX with strongly increased depth, the airflow characteristics (pressure loss at HX) must be carefully taken into account. This is strongly influenced by the fan and the available power to provide high air mass flows.

Figure 10 depicts this conflict for an HX and fan setup with the green lines being the fan's pressure vs. mass flow characteristic for different fan speeds and the blue lines being two differently deep HX pressure loss characteristics.

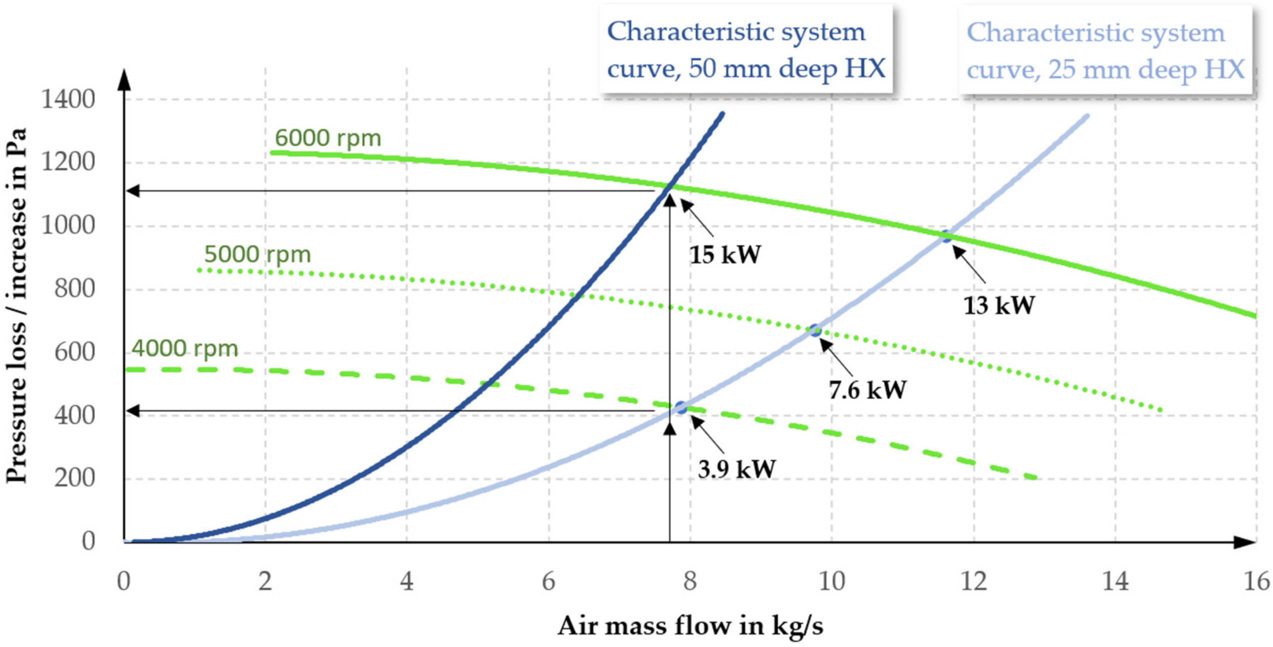


**Figure 10.** Hydraulic Characteristics of 2 HXs in Blue with Constant Speed Fan Curves in Green.

Calculations showed that at doubling the HX depth from 25 to 50 mm, the indicated fan power curves in blue accumulate hugely with exponential behavior. For the same air mass flow, this heads in approximately 1200 Pa instead of 400 Pa pressure loss and 15 kW instead of 3.9 kW electric fan power. This interference depicts a major limitation for the designer of the thermal system. Beyond a system-specific limit in-depth, the extraordinary gain in pressure loss prevails and leads to the too-high electrical power consumption of the fan.

3.1.5. HX Design for MD and HD Truck

With data from Table 1, equations provided in Section 2.3 and diagrams from Section 3, the final design of the HX at appropriate air mass flow can be shaped for the MD and HD truck. At 35 °C ambient temperature, the minimum required air mass flow amounts to 4.3 kg/s for the MD truck and to 8.7 kg/s for the HD truck. By adding a safety margin, this results in 6 kg/s airflow for MD and 12 kg/s airflow for HD, the HX thermal conductance is then calculated with 8400 W/K and 16,800 W/K, respectively. Assuming a cross-sectional area of 1 $m^2$ each, a depth of 25 mm and 45 mm is required to operate FC at full load steady state at 35 °C ambient temperature. Table 4 lists the approximate HX depth for the MD and HD HX for further ambient temperatures for completeness.

**Table 4.** Different HX Depths for 1 $m^2$ HX for MD and HD Truck Applications.

| Ambient Temperature | HX Cross Section Area | MD HX Depth | HD HX Depth |
|---|---|---|---|
| 35 °C | | 25 mm | 45 mm |
| 40 °C | 1 $m^2$ | 45 mm | 85 mm |
| 45 °C | | 75 mm | 145 mm |

### *3.2. Transient Cycle Simulations*

Dynamic driving reveals additional effects and details compared to steady-state considerations. In terms of a thermal system, the inertia of each component is considered, which depends on the mass and specific heat capacity. Higher thermal inertia leads to longer heat-up times of coolant and components. Further, during harsh ambient conditions, components can be operated longer at maximum power before derating is activated. The FC operation is always influenced by such a derating mechanism in order to keep coolant inlet temperatures at defined levels. To evaluate the designed thermal management system in operation with the FC and the PEM (powertrain energy management), transient system simulations are a very helpful and revealing method. Hence, the above-described system with FC and HX is tested and evaluated in transient driving cycles. Therefore, a modular truck simulator is used which is described in the next section.

The target of transient simulations is to show whether the design according to steady state operation is chosen correctly to also withstand critical real driving conditions.

Therefore, two challenging driving cycles are presented in the following which represent typical and challenging transportation routes for an HD truck. The first driving cycle is following the Brenner Highway A10 from Innsbruck (Austria) to Sterzing (Italy), with an 800 m altitude difference making it one of the most demanding HD truck driving routes. The second driving cycle is the VECTO long-haul mission profile from the correspondent European Commission tool [24]. This well-known mission profile to evaluate energy consumption and $CO_2$ emissions of trucks helps to generate comparable results and to provide a more transparent result for interesting groups. The psychrometric properties of air and coolant are based on data from the CoolProp library [25]. For air, an absolute moisture of 9.5 g/kg is assumed, and the coolant properties are based on a water–glycol mixture with 50:50 parts.

#### 3.2.1. Brenner Cycle Results

The Brenner cycle results are summarized for three different ambient temperatures in Figure 11. During the first uphill part, the FC is operated continuously with maximum heat losses of 400 kW. The thermal management requests on the fan and hence air mass flow are strongly increasing with the ambient temperature. The coolant temperature is controlled via fan and thermostat to 62–70 °C with a few runaways, once above the symbolic threshold of 77 °C. This 77 °C–threshold represents the starting of a counter for first derating measures. The thermostat valve (not shown in the graphic) is constantly open between 95–100% during the uphill phase for maximum coolant mass flow. This and the high requests on the fan illustrate a maximum and harsh operation for the system but the thermal management is barely capable of avoiding undesired high temperatures despite the time from 500 s to 800 s. For this specific phase, the FC in combination with the ESS can't provide sufficient power.

During the second downhill part, the FC is shut off, during this phase the ESS can be fully recharged.

#### 3.2.2. VECTO Long-Haul Cycle Results

Figure 12 shows simulation results for a 40 t FC HD truck during the VECTO long-haul mission profile. At 1600 s and 2200 s, long-lasting, and high road gradients require full system power with FC operation at full load. Compared to the Brenner cycle (one FC full load event), with two FC full load events, this cycle is more demanding on thermal management. Required fan power and air mass flow strongly increase with ambient temperature, the fan is operating constantly during these events at 45 °C ambient temperature. Again, the FC derating mechanism is not activated but its operation could be used to drop temperature sufficiently during the two full load events.

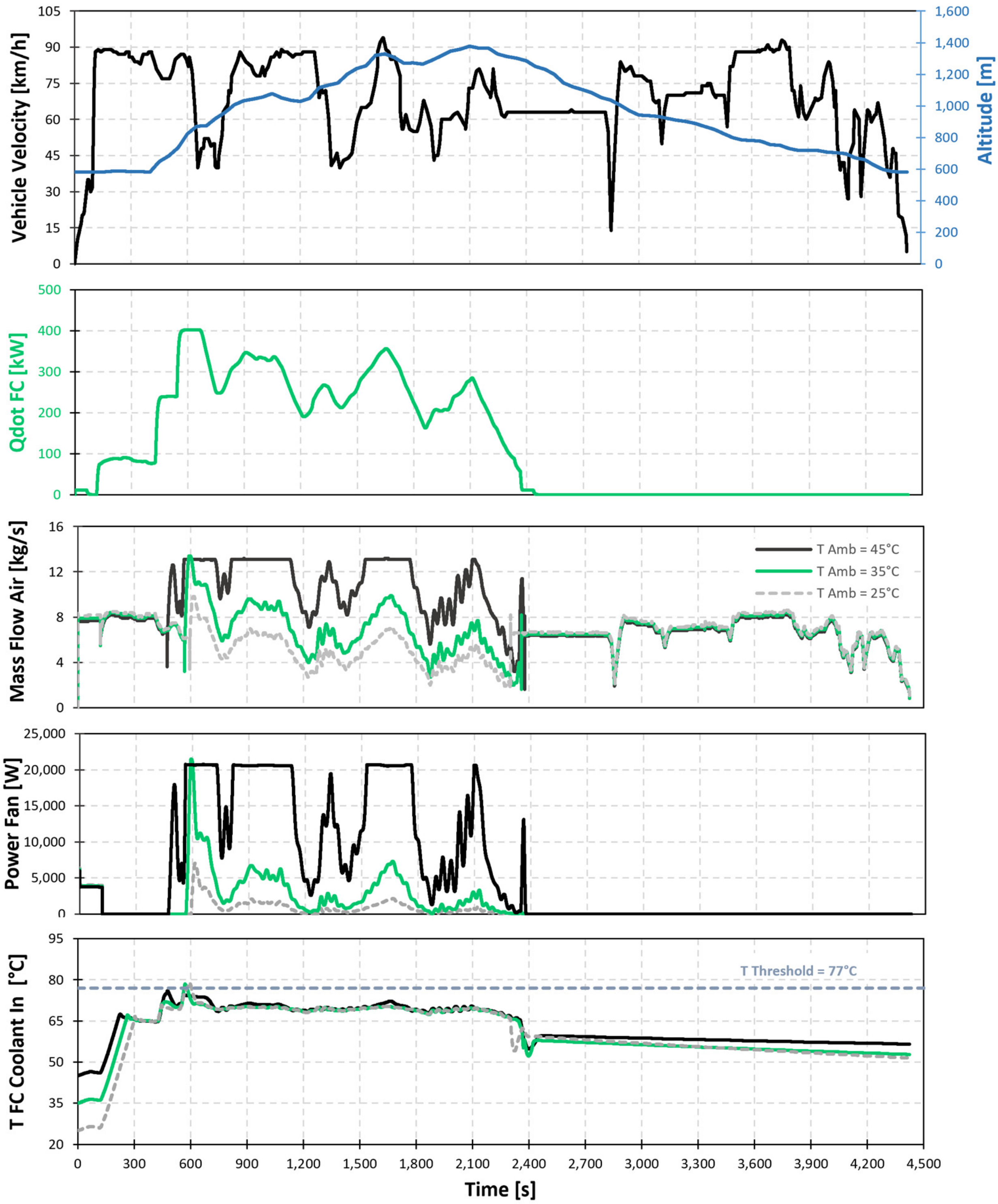


**Figure 11.** Brenner Cycle Results.

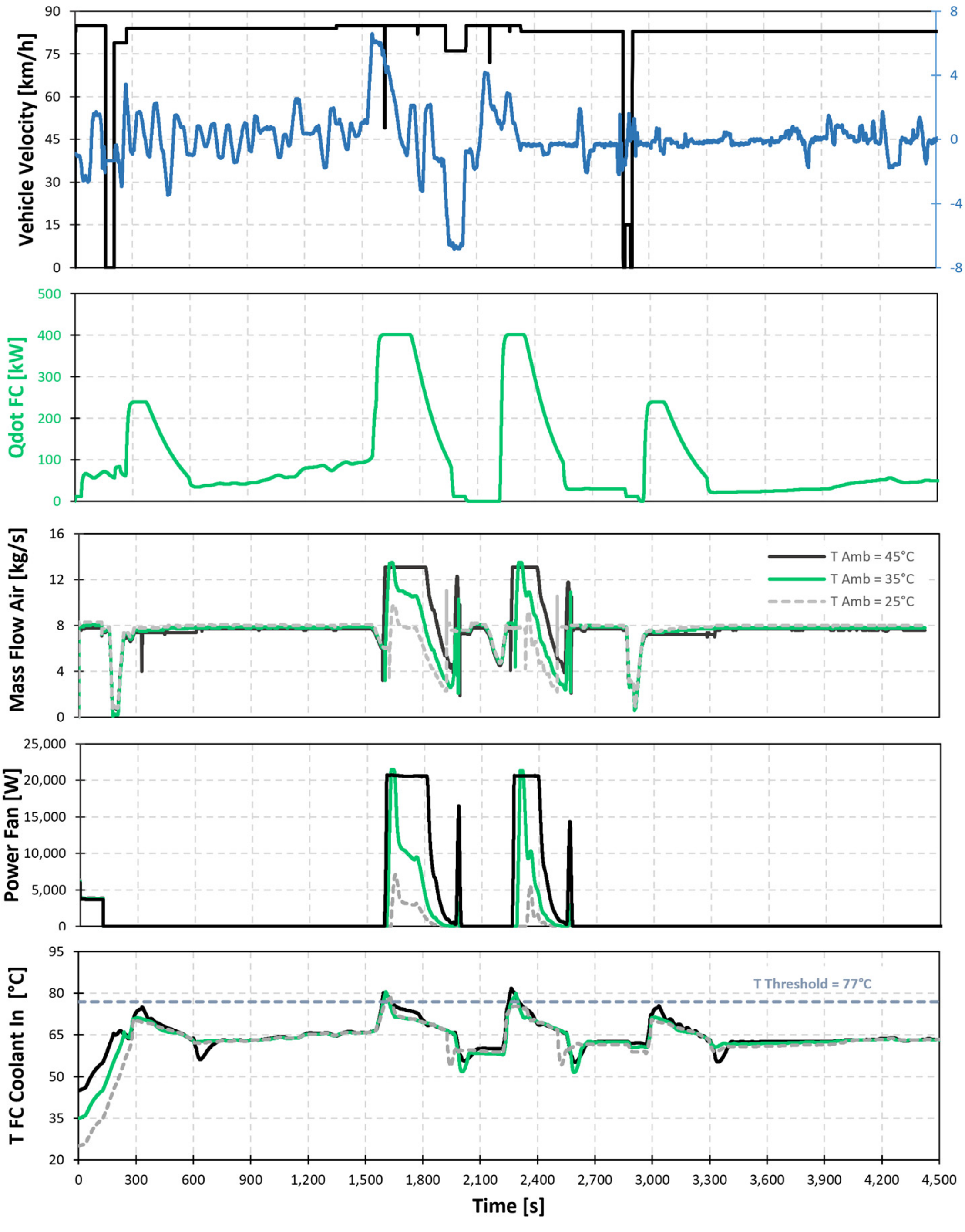


**Figure 12.** VECTO Long Haul Cycle Results.

In general, it can be summarized, that also without the FC derating activation, the thermal management system is designed to dissipate FC heat losses accordingly with only 2 high–temperature events (above 77 °C) lasting longer than 1min in the presented worst-case scenarios. In the next step, with the activation of the FC derating mechanism, such a rare border event can be addressed effectively at the cost of a reduced driving speed. These results, finally, reinforce the purpose of the designed thermal management in the context of the full vehicle system.

## 4. Discussion

This paper presents a guideline to develop an FC cooling system. In the first step, the minimum required air mass flow at the HX was defined to operate the FC at full load in a steady state. In doing so, various HX conductance values were derived as enablers to define HX sizes in the next step. Now, by increasing air mass flow rates, a reduction of the necessary HX size was shown. In the next step, several combinations of cross-sectional area and air mass flow were generated and evaluated. In this scaling process, a maximum feasible air mass flow could be identified in terms of fan power consumption. This point of maximum air flow represents in reverse conclusion the smallest possible HX size to operate the FC at full load in a steady state. Consequently, working ranges of air mass flow and HX sizes were defined extensively, and it is now up to the cooling system designer to accommodate a suitable combination of HX and fan within the available packaging, thus breaking up the heat transfer area in a final step into HX cross-sectional area and HX depth. Usually, there is only a small margin in increasing depth to raise the overall heat transfer area. An excessive increase will no longer necessarily lead to better system performance because either the air-side pressure loss or the fan's power consumption will rise too much.

Further, the effect of ambient temperature on the HX size has been shown. At higher ambient temperatures, the driving force to dissipate heat is reduced. In combination with an increase in desired FC HX size, requirements ascend linearly in the beginning and exponentially in the end. On the one hand, the system designer will come up soon against limitations with available packaging. On the other hand, a stronger fan can help to move into the area with linear surface growing behavior, so less HX size is required. In this way, careful consideration of natural airflow by driving velocity and forced airflow is crucial. Instead of designing the HX for FC operation at full load in a steady state, the HX can also be designed for lower loads in a steady state, e.g., for 80% or 90%. This work showed that in this way the HX size can be drastically reduced to only 55% or 75% in size. These strong reductions can be constituted due to the exponential growing behavior at high loads. At the same time, this leads to less required air mass flow and lower fan size.

Finally, for MD and HD trucks, the HX sizes were chosen with 1 $m^2$ cross-sectional area both and depths of 25 mm and 45 mm, respectively; this correlates to FC full load operations in a steady state at 35 °C. The performance of the fan was limited to max. 22 kW power and to the max. 12 kg/s air mass flow for the HD truck; for the MD truck values are halved. In the final step, the system was validated in transient simulations. Target coolant temperatures were mostly reached, only in very few harsh mission profiles, minor overshooting up to 1 min was observed. To avoid such an event, the FC derating mechanism can be activated, hence this will influence the matching of desired vehicle velocity.

## 5. Conclusions

In the introduction, Section 1, information is collected on state-of-the-art thermal management systems for FC trucks. It constitutes a comprehensive collection of detailed information on thermal parameters which has not been available so far. This paper presents for the first time such an overview in literature, thanks to this, it provides a good starting point for the cooling system developer to estimate thermal system dimensions. Subsequently, a structured novel methodology was presented to choose the HX. Due to the low installation space for the HX and the high fan power demands, integration, and efficient operation are of exuberant importance. The non-linear increase of HX size was not reported to that extent in any literature which is especially crucial for FCs. With this publication, a novel layout process is proposed to treat reported trade-offs. The described procedure can be used by a cooling system developer for any type of FC with adaptations in parameters. Because of the described lack of information on such a structured thermal management system process so far, this publication can make a considerable contribution to pushing the hydrogen movement.

**Author Contributions:** Both authors contributed in the same way to this publication with concept evaluations, system modelling, simulation activities, and writing. All authors have read and agreed to the published version of the manuscript.

**Funding:** This project has received funding from the Mobility of the Future programme. Mobility of the Future is a research, technology and innovation funding programme of the Republic of Austria, Federal Ministry for Climate Action (BMK). The Austrian Research Promotion Agency (FFG) has been authorized for the programme management. The publication was written at Virtual Vehicle Research GmbH in Graz and partially funded within the COMET K2 Competence Centers for Excellent Technologies from the Austrian Federal Ministry for Climate Action (BMK), the Austrian Federal Ministry for Digital and Economic Affairs (BMDW), the Province of Styria (Dept. 12) and the Styrian Business Promotion Agency (SFG). The Austrian Research Promotion Agency (FFG) has been authorised for the programme management.

**Data Availability Statement:** Not applicable.

**Acknowledgments:** The work was carried out in the NextGenFCM project. Data and models for the FC are based on this project work with HyCentA Research GmbH and Plastic Omnium New Energies Wels GmbH.

**Conflicts of Interest:** The authors declare no conflict of interest. The funders had no role in the design of the study; in the collection, analyses, or interpretation of data; in the writing of the manuscript; or in the decision to publish the results.

## Abbreviations

| | |
|---|---|
| BoP | Balance of Plant |
| BOL/EOL | Begin Of Life/End Of Life |
| ESS | Energy Storage System |
| FC | Fuel Cell |
| GVW | Gross Vehicle Weight |
| HD | Heavy Duty |
| HV | High Voltage |
| HX | Heat Exchanger |
| ICE | Internal combustion engine |
| MD | Medium Duty |
| PEM | Powertrain Energy Management |
| PEMFC | Polymer Electrolyte Membrane Fuel Cell |
| SOC | State Of Charge |
| VECTO | Vehicle Energy Consumption calculation Tool |

**Nomenclature**

| | | |
|---|---|---|
| $\dot{Q}$ | Thermal Dissipation, Heat Flow | W |
| $A_{HX}$ | Heat Exchanger Heat Transfer Area | $m^2$ |
| k | overall heat transfer coefficient | $W\,m^{-2}\,K^{-1}$ |
| $\overline{T}$ | Mean Temperature | °C |
| $\dot{m}$ | Mass Flow | $kg\,s^{-1}$ |
| $c_p$ | specific Heat Capacity at constant pressure | $J\,kg^{-1}\,K^{-1}$ |
| $\Delta T$ | Temperature Difference | K |
| T | Temperature | °C |
| o, out | property at outlet | |
| i, in | property at inlet | |
| c, coolant | coolant side of Heat Exchanger | |
| a, air | air side side of Heat Exchanger | |
| th | thermal | |

## References


1. Pardhi, S.; Chakraborty, S.; Tran, D.-D.; El Baghdadi, M.; Wilkins, S.; Hegazy, O. A Review of Fuel Cell Powertrains for Long-Haul Heavy-Duty Vehicles: Technology, Hydrogen, Energy and Thermal Management Solutions. *Energies* **2022**, *15*, 9557. [CrossRef]
2. Schnorpfeil, S.; Hartmann, E.; Kotowski, A.; Kapadia, B.; Sötje, H. *Fuel Cell Propulsion System Layout*; ATZ Der Antrieb von morgen; Springer: Berlin/Heidelberg, Germany, 2021; p. 8.
3. Berger, O. Thermodynamische Analyse Eines Brennstoffzellensystems zum Antrieb von Kraftfahrzeugen. Ph.D. Thesis, Universität Duisburg-Essen, Essen, Germany, 2009.
4. Godard, K.; Chauvin, L. Hydrogen Powertrain Designs for European Long-Haul Trucks. In Proceedings of the 30th Aachen Colloquium Sustainable Mobility, Aachen, Germany, 4–6 October 2021; pp. 82–84.
5. Aschauer, T.; Schutting, E.; Eichlseder, H. Hydrogen Powered Telehandler Concept. In Proceedings of the 43rd International Vienna Motor Symposium, Vienna, Austria, 27–29 April 2022.
6. Mayr, K.; Hofer, F.; Ragowsky, G.; Gruber, W.; Arnberger, A.; Kabza, A.; Wolf, P.; Schmidt, M.; Jörissen, L. *Systemvergleich Zwischen Wasserstoffverbrennungsmotor und Brennstoffzelle im Schweren Nutzfahrzeug*; e-mobil BW Study: Stuttgart, Germany, 2021.
7. Linderl, J.; Mayr, J.; Döbereiner, R. Integration of a Fuel Cell Powertrain for a 4 × 2 Heavy Duty Truck. 2021. Available online: https://www.grcc.vip/article-8669.html (accessed on 1 March 2023).
8. Buyens, N. Fuel Cell Mobility: Toyota Strategy & Thermal Challenges. In Proceedings of the Advanced Thermal Management in Future: Hydrogen Fuel Cell Powered Vehicles Webinar, Online, 8 June 2021; Institution of Mechanical Engineers: London, UK, 2021.
9. Fraser, N. Challenges & Solutions for Fuel Cell Vehicle Thermal Management Systems. In Proceedings of the Advanced Thermal Management in Future: Hydrogen Fuel Cell Powered Vehicles Webinar, Online, 8 June 2021; Institution of Mechanical Engineers: London, UK, 2021.
10. Pietruck, M.; Massonet, C.; Backes, D. Predictive and Heat-Managed Operating Strategy for a Fuel Cell Electric Vehicle. In Proceedings of the 30th Aachen Colloquium Sustainable Mobility, Aachen, Germany, 4–6 October 2021.
11. Roiser, S. *Thermal Management of a Heavy-Duty Truck with Fuel Cell Drive*; KULI-Webinar: Linz, Austria, 2021.
12. Linderl, J.; Mayr, J.; Hütter, M.; Döbereiner, R. Optimized Fuel Cell Drive for Long-haul Trucks. *ATZheavy Duty Worldw.* **2021**, *14*, 38–43. [CrossRef]
13. Kwon, H.; Park, S.; Choi, J.; Han, J. A Study on the Optimization of the Louver Fin Heat Exchanger for Fuel Cell Electric Vehicle Using Genetic Algorithm. *Appl. Sci.* **2023**, *13*, 2539. [CrossRef]
14. Engineering Center Steyr. KULI Software Trial Version 16.1; HX Component Measurement Data. Available online: https://kuli.magna.com/ (accessed on 17 March 2023).
15. Vijayagopal, R. Analysis of Fuel Cells for Trucks, Argonne National Laboratory. In Proceedings of the 2019 DOE Hydrogen Program and Vehicle Technologies Annual Merit Review, Washington, DC, USA, 29 April–1 May 2019.
16. FIC-31 HV Fan. EMP, 7 September 2022. Available online: https://www.emp-corp.com/product/fic-31-high-voltage-fan/ (accessed on 15 March 2023).
17. WP150 HV Pump. EMP, 14 July 2022. Available online: https://www.emp-corp.com/product/wp150-high-voltage/ (accessed on 15 March 2023).
18. Borgwarner Secures First High Voltage E-Fan System Win, BorgWarner. Available online: https://www.borgwarner.com/newsroom/press-releases/2022/02/15/borgwarner-secures-first-high-voltage-efan-system-win (accessed on 17 March 2023).
19. Kühlmittelpumpen, Rheinmetall. Available online: https://www.rheinmetall-automotive.com/systeme-produkte/pkw/pumpen/kuehlmittelpumpen/ (accessed on 17 March 2023).
20. Rama, P. Jaguar Land Rover. Project Zeus Thermal Management. In Proceedings of the Thermal Management in Future: Hydrogen Fuel Cell Powered Vehicles Webinar, Online, 8 June 2021; Institution of Mechanical Engineers: London, UK, 2021.
21. Nissens Nis 606322 Front End HX for Scania S. Available online: https://www.motointegrator.at/artikel/1804134-kuehler-nissens-nis-606322 (accessed on 17 March 2023).
22. AVA VL2148 Front End HX for Volvo FH16. Available online: https://www.motointegrator.at/artikel/1476467-kuehler-motorkuehlung-ava-cooling-vl2148 (accessed on 17 March 2023).
23. AVA Engine HX MN2088 for MAN TGX. AVA. Available online: https://www.ava-cooling.com/katmod1.php?xart=MN2088 (accessed on 17 March 2023).
24. European Comission. Vehicle Energy Consumption Calculation Tool—VECTO. Available online: https://climate.ec.europa.eu/eu-action/transport-emissions/road-transport-reducing-co2-emissions-vehicles/vehicle-energy-consumption-calculation-tool-vecto_en (accessed on 17 March 2023).
25. Bell, I.H.; Wronski, J.; Quoilin, S.; Lemort, V. Pure and Pseudo-pure Fluid Thermophysical Property Evaluation and the Open-Source Thermophysical Property Library CoolProp. *Ind. Eng. Chem. Res.* **2014**, *53*, 2498–2508. [CrossRef] [PubMed]